Sustainable Engineering Materials
ISSN: 3105-1960 (Print); ISSN: 3105-1979 (Online)
http://www.sustain-dpl.com/picnews.asp?id=177
DOI: 10.54113/j.suem.2026.000014

REVIEW ARTICLE

Mechanical and durability properties of ultra-high-performance concrete of spent nuclear fuel dry storage systems: a review

Mohamed T. Elshazli[a], Elmar Eidelpes[b], Gabriel O Ilevbare[c], Ahmed Ibrahim[d,*]

[a]Assistant Research Professor, Department of Civil and Environmental Engineering, University of Missouri, Columbia, MO 65201, United States
[b]Former Spent Fuel Analyst, Used Fuel Management Department, Nuclear Science and Technology, Idaho National Laboratory, Idaho Falls, ID 83415, United States
[c]Materials Science and Manufacturing Department, Energy and Environment Science and Technology, Idaho National Laboratory, Idaho Falls, ID 83415, United States
[d]Professor, Department of Civil and Environmental Engineering, University of Idaho, Moscow, ID 83844-1022, United States
[*]Corresponding Author: Ahmed Ibrahim. Email: aibrahim@uidaho.edu

Abstract: Dry storage systems are used for interim storage of spent nuclear fuel (SNF). However, with the growing need to extend the operational periods of these systems, there are concerns about the degradation of their concrete overpacks, which could compromise the system's structural integrity and safety during hazardous events. Traditional concrete mixtures used in SNF dry storage systems have remained largely unchanged since their inception and often use conventional ingredients. These materials are susceptible to degradation mechanisms such as chemical attacks, alkali-silica reactions (ASR), and freeze–thaw cycles, which can lead to a loss of strength and durability over time. To address these challenges, this paper reviews the application of ultra-high-performance concrete (UHPC) as a promising alternative for spent nuclear fuel dry storage system overpacks. UHPC offers superior mechanical properties, exceptional durability, and reduced susceptibility to degradation mechanisms compared to conventional concrete. This paper focuses on the role of supplementary cementitious materials (SCMs) such as silica fume, fly ash, and metakaolin in enhancing UHPC performance for SNF storage applications. These SCMs have been shown to significantly improve the material's microstructure, strength, and resistance to environmental stressors typically encountered in SNF storage environments. Moreover, incorporating SCMs supports sustainable construction by reducing cement consumption and associated carbon emissions. The review brings together existing research and experimental data, providing insights for engineers and researchers on developing UHPC mixtures that meet the rigorous demands of spent nuclear fuel dry storage systems, extending their service life and minimizing inspection intervals.

Keywords: UHPC, concrete, spent nuclear fuel (SNF)

1 Introduction

The safe and long-term disposal of radioactive waste remains a critical challenge for the nuclear industry, as demanding engineering requirements must be met to prevent environmental contamination and structural degradation [1, 2]. Following reactor discharge, spent nuclear fuel (SNF) is initially

Received: 30 August 2025; Received in revised form: 4 February 2026; Accepted: 8 February 2026

stored in water-filled pools for cooling. However, due to the limited capacity of these pools, alternative storage solutions became necessary. Consequently, dry cask storage (DCS) systems were introduced in the mid-1980s as an interim solution [3, 4]. A permanent geological repository at Yucca Mountain, Nevada, was initially proposed in 1986, but its future remains uncertain due to political and technical challenges [5]. In the absence of a permanent disposal facility and the lack of fuel reprocessing, dry storage remains the primary method for managing SNF in the U.S. The Nuclear Energy Institute projects that the total amount of SNF will more than double, reaching 140,000 metric tons by 2055 [6], necessitating the long-term reliability of dry cask storage.

Concrete DCS systems for SNF typically consist of a metal canister that is enclosed within a concrete overpack, as shown in **Fig. 1**. Depending on site constraints and design considerations, these casks can be positioned either vertically or horizontally [7]. In concrete overpack designs, the shielding envelope may consist of reinforced concrete, concrete with an inner steel liner, or a hybrid configuration featuring both inner and exterior steel liners with a concrete-filled core [8]. While concrete has a lower density compared to metal, requiring thicker shielding components, it is highly effective in attenuating gamma rays and slowing down fast neutrons, making it a viable material for radiation protection [9]. Furthermore, the thermal properties of concrete contribute to the dissipation of decay heat from the SNF, ensuring the long-term stability of the storage system.

Available literature has documented various cases of concrete degradation in nuclear power plant structures and dry cask storage systems. For example, in the Three Mile Island (TMI) storage casks, freeze-thaw cycles trapped water in bolt-hole voids, causing cracks in the concrete roof slabs [9, 10]. Degradation mechanisms identified in our previous study—driven by factors such as chemical attacks, alkali-silica reaction (concrete cancer), and freeze-thaw (F-T) cycles—pose a significant risk to the structural integrity of storage modules, particularly during long-term dry storage or seismic events [9]. Traditionally, the concrete mixtures utilized in these systems have seen little evolution, often utilizing the same compositions as of conventional concrete. However, recent advances in material science present numerous potentials to improve the performance of these structures.

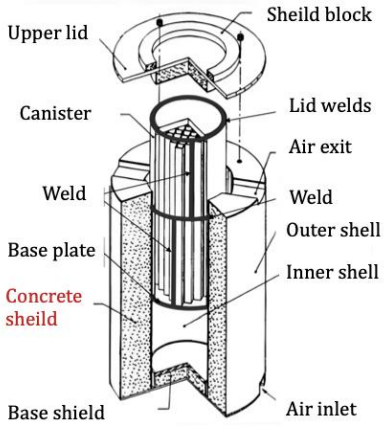

Fig. 1. A representation of the continuous particle packing model

By utilizing advanced concrete mixtures developed in the past decade, SNF structures can achieve improved durability and mechanical performance, whether applied in new construction projects or in the rehabilitation of existing concrete elements [11]. Ultra-high-performance concrete (UHPC) is among the concrete materials that have demonstrated superior mechanical properties and remarkable long-term durability [12, 13]. Recently, UHPC has emerged as a highly promising construction material with enormous potential to advance the future development of resilient and sustainable infrastructure [14–18].

UHPC represents a recent advance in cementitious materials characterized by exceptional strength, ductility, and durability [19]. Despite the interchangeability of the terms high-performance concrete (HPC) and high-strength concrete (HSC), there is a significant difference between them [20]. Concrete strength alone does not guarantee durability. UHPC, especially when reinforced with fibers, can be considered as a combination of three concrete technologies: self-compacting concrete (SCC), fiber-

reinforced concrete (FRC), and high-performance concrete (HPC) [21, 22]. For UHPC, numerous definitions have been introduced. The American Concrete Institute (ACI) defines UHPC as concrete that satisfies specialized combinations of performance and uniformity requirements, often unattainable through conventional constituents and normal mixing, placing, and curing practices [20]. According to UK standards, UHPC improves features such as placement and compaction without segregation, long-term mechanical properties, early age strength, toughness, and volume stability in harsh environments [20]. French interim recommendations (AFGC 2002) define UHPC as concrete reinforced with fibers that can achieve a compressive strength of at least 150 MPa [23].

The research presents a comprehensive review of recent advances in UHPC and investigates its potential to enhance mechanical and durability properties, thereby offering a viable solution for extending the service life of DCS's concrete overpack. By addressing the primary degradation mechanisms identified in our previous research [9]—including freeze-thaw (F- T) cycles, alkali-aggregate reaction (AAR), reinforcement corrosion, and radiation-induced damage—UHPC's superior resistance to environmental and chemical stressors makes it a promising material for mitigating deterioration and ensuring the long-term structural integrity of spent nuclear fuel storage systems.

2 The development of UHPC

The goal of UHPC mixtures is to create a densely compacted cementitious matrix with good workability and strength [24]. Most publications provide the proportions of UHPC mixtures without providing any design procedures or explanation. However, two design models were developed in the literature: the particle packing model and the performance model. **Fig. 2** shows a representation of a continuous particle packing model. The high particle packing density is achieved in the particle packing model by introducing particle size distributions P(D), which contribute to low porosity, high mechanical strengths, and impermeability [25–27]. The modified Andersen and Andreasen model [28–30] are the most widely used target function for optimizing the composition of a mixture of granular materials, using **Eq. (1)**.

$$P\left(D_i\right)=\frac{D_i^q-D_{\min}^q}{D_{\max}^q-D_{\min}^q} \tag{1}$$

Where *P(Di)* represents the proportion of total solids that have a size smaller than *Di*, D_{max} and D_{min} are the maximum and minimum particle sizes (in units of μm), respectively, and q signifies the distribution modulus.

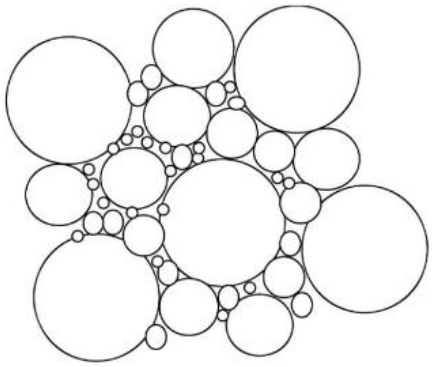

Fig. 2. A representation of the continuous particle packing model

Eq. (1) can be used to design UHPC through the application of different distribution moduli q, which govern the ratio of fine to coarse particles in the mixture. The *q* value for UHPC was suggested to be in the range of 0.21-0.25 [24, 31]. Hunger, (2010) [32] and Yu et al., (2015) [33] suggested employing a q value of 0.23 in UHPC to ensure a substantial quantity of fine particles [34]. Using an optimization process based on the Least Squares Method (LSM), **Eq. (2)**, the proportions of each individual constituent in the mixture are modified until an optimum match between the constructed mixture and the target curves is achieved. This model has been utilized and verified using experimental work.

$$RSS = \sum_{i=1}^{n} \left[P_{mix}\left(D_i\right) - P_{tar}\left(D_i\right)^2 \right] \quad (2)$$

where P_{mix} is the constructed mixture, and P_{tar} is the target grading calculated from Equation 1.

The packing density of particles in the Andersen and Andreasen model is based on dry conditions, which may not accurately represent the packing density of particles in UHPC due to the impact of water and other liquids [35]. The presence of water can reduce friction force. The force can be removed when the fine particles are saturated [36]. As a result, the wet particle packing model achieves a higher particle packing density than the dry packing model. A high wet packing density improves the macro-meso-micropore structure of UHPC and compressive strength [37]. To obtain the maximum packing density, solid concentrations (φ) and void ratios (u) are optimized using **Eq. (3) – (5)** [24].

$$V_c = \frac{M}{\rho_w u_w + \rho_\alpha u_\alpha + \rho_\beta u_\beta + \rho_\gamma u_\gamma} \quad (3)$$

$$u = \frac{V - V_c}{V_c} \quad (4)$$

$$\varphi = \frac{V_c}{V} \quad (5)$$

Where M and V represent the mass and volume of paste, respectively, in a cylindrical mold with 62 mm diameter and 60 mm height; ρw denotes the density of water; $\rho\alpha$, $\rho\beta$, and $\rho\gamma$ represent the solid densities of various cementitious materials; and $R\alpha$, $R\beta$, and $R\gamma$ represent the volumetric ratios of the different cementitious materials.

The maximum packing density does not necessarily result in the best UHPC performance; therefore, the performance-based method was developed. Meng et al. (2017) [38] proposed a performance-based approach to optimize UHPC mixtures. The approach considers particle packing, workability, and mechanical properties. Based on the relationship established between the variables and the target performance, the mixture design parameters such as the water-to-binder ratio (w/b), fiber content, and binder-to-sand ratio can be directly and correctly determined.

Over the last three decades, the evolution of UHPC can be traced through different stages. Initially, high-strength concrete (HSC) was produced in laboratories using vacuum mixing and heat curing. Then, micro-defect free cement (MDF) was introduced, enabling the development of UHPC with compressive strength exceeding 200 MPa. However, high material costs and complicated production techniques limited its utilization. Subsequently, in Denmark, dense silica particle (DSP) cement was developed to enhance concrete's particle packing density, offering a more accessible production method than MDF cement. By incorporating silica fume, superplasticizer, and employing pressure curing conditions, DSP-incorporated concrete achieved an impressive maximum compressive strength of 345 MPa. Steel fibers were added to this concrete to reduce brittleness. These advancements produced slurry infiltrated fiber concrete (SIFCON) with up to 20% steel fibers by volume. SIFCON's lack of workability limited its use, despite its flexural strength of 25–70 MPa.

3. Typical ingredients of UHPC

UHPC is typically made using a combination of high-quality materials to achieve exceptional strength and durability. A typical UHPC formulation incorporates high-strength Portland cement as the primary binder, supplemented by silica fume to enhance overall strength [39–42]. Fine aggregates, such as finely graded sand or quartz powder, contribute.

to the dense and compact structure of concrete [43–45]. Superplasticizers are used to improve workability without compromising strength, while steel or polymer fibers are used to increase tensile strength and toughness [46–48]. Chemical admixtures can also be used to achieve specific properties, such as accelerators or retarders, to control set time [49, 50]. Furthermore, recent research incorporated nanomaterials, such as nano-silica, nano-alumina, and carbon nanotubes, which represents a cutting-edge strategy to enhance the material properties [51– 53]. These nanomaterials contribute to improved strength, durability, thermal resistance, and improved electrical conductivity [54–56]. The proportions

and types of these ingredients can vary to tailor the UHPC mix to specific performance requirements, and ongoing research may introduce new materials or modifications for further enhancement.

The cement content in UHPC typically ranges from 800 to 1000 kg/m^3 [39, 57, 58], enabling the material to achieve its ultra-high strength and dense microstructure. However, this high cement dosage significantly increases production costs and also influences hydration heat and dimensional stability [33, 59, 60]. The elevated heat of hydration can create thermal gradients within the concrete matrix, raising the risk of early-age cracking. Additionally, the high cement content can lead to substantial autogenous shrinkage, which may compromise the dimensional stability of the UHPC. Previous studies have recommended the use of ASTM Type I or II cements for UHPC [39, 57] due to their balanced hydration characteristics and moderate heat evolution. To address the cost and sustainability challenges associated with high cement use, Portland cement is increasingly being partially substituted with supplementary cementitious materials (SCMs) such as silica fume (SF), fly ash (FA), granulated blast furnace slag (GGBFS), and metakaolin (MK), which enhance the overall efficiency and performance of UHPC.

4. Mechanical properties

Numerous studies have been conducted to identify optimal mixture proportions and assess the mechanical properties of UHPC [58, 61–64]. A wide range of approaches are used to improve the mechanical properties of concrete, including the use of supplementary cementitious materials, optimizing concrete design, incorporating fine minerals, and integrating fibers. This section provides a comprehensive review of the effects of various parameters on the mechanical properties of UHPC.

4.1. Supplementary Cementitious Materials (SCMs)

Supplementary Cementitious Materials (SCMs), such as silica fume (SF), fly ash (FA), metakaolin (MK), and ground granulated blast furnace slag (GGBFS), have been extensively used to improve the mechanical properties of concrete [65]. **Table 1** summarize the key findings from previous research work.

Silica fume (SF) is a widely used SCM that has been increasingly adopted for the last thirty years. Incorporating SF has been shown to speed up the hydration process, resulting in significant increases in concrete strength development [65]. Various studies explored different SF contents ranging from 0% to 35% [19, 66]. It has been consistently reported that the optimal replacement of Ordinary Portland Cement (OPC) with SF is around 10% [67–69]. Moreover, exceeding a replacement rate of 20% has been found to have negligible effect. From a cost perspective, SF is generally more expensive than traditional cement due to its limited availability and the processing required for use in concrete. However, its high reactivity allows for lower dosages compared to cement, which can offset some of the cost increase at the mixture level. In addition, the use of SF contributes to environmental sustainability because it is an industrial byproduct of silicon and ferrosilicon alloy production. Diverting SF from landfilling reduces waste, lowers the demand for clinker production, and decreases the carbon footprint of UHPC mixtures. Therefore, although SF increases unit material costs, its environmental benefits and contribution to long-term durability and reduced maintenance costs make it a cost-effective and sustainable choice for UHPC in critical applications such as spent nuclear fuel storage.

Fly Ash (FA) is a byproduct from coal power plants. Typically, it is mixed with GGBFS, SF, and/or steel slag powder (SS) in binary, ternary, or quaternary systems [70, 71]. The combination of GGBFS and FA has been found to increase flexural strength and significantly improve concrete toughness under varied curing conditions [72–74]. However, it tends to reduce the modulus of elasticity, especially when the cement replacement exceeds 30%.

Metakaolin (MK) is made by calcining natural clay. Its pozzolanic reactivity is primarily influenced by the calcining temperature [75]. Metakaolin powder has been demonstrated to reduce autogenous shrinkage, refine pore structure, and increase early strength in concrete [75–77]. The optimal MK content has been consistently reported between 10% and 15% [78–80].

Granulated blast furnace slag (GGBFS) has been used as a supplementary cementitious material in concrete for many years. Replacing cement with GGBFS resulted in increased strength up to a certain replacement content limit. Optimum replacement was identified at 10% [81–83]. When used as a

replacement for Portland cement at varying pro- portions and water to cement ratio (w/c) ratios of 0.4 and 0.45, GGBFS exhibited improved strength after 28 days of curing. However, at a w/c ratio of 0.4, strength decreased at 7 days compared to a w/c ratio of 0.45. A replacement level of 30% was determined to be optimal for both w/c ratios of 0.40 and 0.45 [84].

4.2. Water-to-Binder (w/b) Ratio

The water-to-binder ratio has a considerable impact on the mechanical properties of UHPC [65]. To achieve the desired mechanical and durability properties, the water-to-binder ratio in HPC should be kept low. Several investigations have used a variety of water-to-binder ratios, including 0.4 [100, 101], 0.35 [101], 0.3 [102], 0.27 [103], 0.25 [104],0.18 [105], and 0.15 [106]. Studies have shown that as the water-to-binder ratio decreases, the strength of concrete typically increases [107–109]. A study [110] on HPC mix proportioning concluded that increasing the binder content while maintaining the effective water-to-binder ratio and water content can help overcome the difficulty of producing slower early-age strength. Furthermore, the increase in the compressive strength was found to be more dependent on the water-to- binder ratio than on silica fume [109]. In terms of optimum values [100-109], most studies on UHPC report that w/b ratios in the range of 0.18–0.25 provide the best balance between compressive strength and durability. Ratios below 0.18 may enhance strength but significantly increase autogenous shrinkage and cracking risk, while ratios above 0.25 generally reduce density and long-term durability. Therefore, an optimum w/b of approximately 0.20–0.22 is often recommended for UHPC to ensure both high strength and resistance to durability-related degradation mechanisms. Thus, it can be concluded that the water-to-binder ratio is one of the key factors causing strength variation in HPC.

4.3. Aggregate

High strength aggregate should be used to develop UHPC. Various types of aggregates have been used in concrete manufacturing, ranging from lightweight [91, 111, 112] to recycled aggregates [106, 113, 114]. According to research, high quality aggregates that are free of alkali-aggregate reactivity are essential to produce HPC [65]. The majority of research recommended the utilization of fine aggregates to decrease the porosity of concrete, thereby enhancing its mechanical and durability properties, **Fig. 3**. Initially, refined quartz sand with a diameter less than 0.6 mm was employed in early UHPC formulations to achieve superior performance, despite its high cost [39]. However, to mitigate the expense associated with UHPC production, alternative materials such as recycled glass cullet, natural sands, and artificial aggregates have been investigated as replacements for refined quartz sand [115, 116].

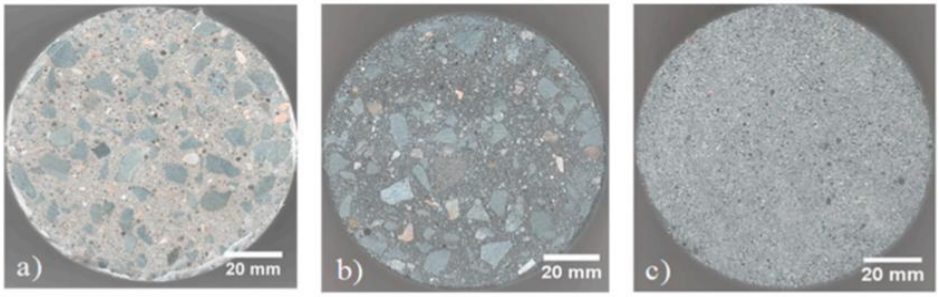

Fig. 3. Cross-sectional views of normal concrete (NC), high-performance concrete (HPC), and ultra-high-performance concrete (UHPC) cylinders [119]

A previous study [117] used crushed basalt with a diameter less than 8 mm to partially replace refined quartz sand in UHPC. Similarly, another study [118] used crushed basalt and limestone with diameters less than 20 mm as coarse aggregates and reported promising results. Specifically, these replacements reduced the overall material cost while maintaining compressive strengths above 150 MPa and flexural strengths exceeding 20 MPa. The use of basalt aggregate improved the interfacial transition zone (ITZ) due to its rough surface texture, enhancing bond strength, while limestone contributed to improved workability and reduced autogenous shrinkage. In both cases, durability indicators such as

resistance to chloride penetration and freeze–thaw cycles were comparable to or better than mixtures containing refined quartz sand, making these alternatives attractive for more economical and sustainable UHPC production.

Table 1. Sample of prior research on the effect of SCMs on the strength of UHPC

CONSTITUENT SUMMARY	REFERENCES
SILICA FUME (SF)	The optimal SF content, which maximizes bonding and compressive strength in UHPC, depends on the water-to-cement (w/c) ratio. Lower w/c requires lower silica fume content [85]. SF concrete composite strength exceeds SF paste strength, deviating from conventional concrete trends [86]. A 21% increase in compressive strength was observed as SF content increased from 0% to 15% [87]. SF has no significant effect on split tensile strength [88]. Some studies report tensile strength reduction at high temperatures [89]. SF has a pronounced effect on flexural strength compared to splitting tensile strength, with most studies reporting a greater relative increase in flexural strength due to the improved bond at the paste–aggregate and paste–fiber interfaces [90]. Elastic modulus of SF concrete matches conventional concrete at 28 days but continues to rise with age [88].
FLY ASH (FA)	FA can be used to produce lightweight HPC [91]. A 22% weight reduction was achieved alongside a 20% increase in compressive strength [91]. Combining GGBFS and FA improves flexural strength and concrete toughness [39]. For instance, studies have shown that binary and ternary blends with 10–20% GGBFS and 15–25% FA (as partial cement replacement) can increase flexural strength by approximately 10–20% and enhance fracture toughness by up to 30% compared to control mixtures. Beyond these levels, the improvements diminish, and excessive replacement may reduce early-age strength. The combination of GGBFS and SF should not exceed 30% of cement content to avoid modulus of elasticity loss [72].
METAKAOLIN (MK)	Three primary factors influence MK's contribution: immediate filler effect (accelerating hydration), pozzolanic reaction (peaks within 14 days), and age strength (no enhancement beyond 14 days) [92, 93]. Replacing 5% OPC with MK increased compressive strength by ~7% [94]. Using 15% MK optimally enhanced compressive strength (~22% increase) [80]. Replacing SF with MK reduced compressive strength by ~7% [95]. High temperature curing of MK concrete increases early strength [96]. This enhancement is attributed to accelerated pozzolanic reactions of MK and faster hydration kinetics under elevated temperatures. For example, curing at 60–80 °C has been reported to increase 7-day compressive strength by 15–25% compared to specimens cured at ambient conditions, while also refining pore structure and reducing permeability. However, excessively high curing temperatures (>90 °C) may cause microcracking and negatively affect long-term strength development. MK is favored for its affordability and availability over other SCMs [39]. Compared to SF, which is a byproduct of silicon and ferrosilicon alloy production and is limited to regions with such industries, MK is produced from abundant natural kaolinite clays available worldwide. Production costs of MK are typically 20–40% lower than silica fume on a per-ton basis, and its supply chain is less restricted, making it more consistently available in both developed and developing regions.

4.4. Fibers

Fibers are commonly integrated into concrete to bridge cracking and enhance strength properties. Research indicates that while the addition of a single type of fiber to HPC may improve specific aspects, optimal performance is often achieved by incorporating various types of fibers [120, 121]. The introduction of fibers transforms the brittle failure of into a more ductile behavior [122–124], see **Fig. 4**. A range of fiber types, including steel, basalt, synthetic, and polypropylene fibers, have been studied.

Table 2 provides a summary of the key findings regarding the utilization of fibers in UHPC. In addition to fiber type and content, fiber length plays a critical role in ductility. Shorter fibers (<10 mm) are more effective at controlling microcracks and improving post-cracking stiffness, but they provide limited pull-out resistance. Longer fibers (13–20 mm for steel and basalt fibers) enhance crack-bridging capacity and energy absorption, resulting in higher ductility and toughness indices. However, excessively long fibers may cause fiber balling during mixing and reduce workability, which can compromise uniform dispersion. Studies generally report that optimum fiber lengths for UHPC are around 13 mm for steel fibers and 12–18 mm for basalt fibers, balancing workability and ductility improvements.

Unlike conventional reinforced concrete, where rebar corrosion can propagate and cause significant structural deterioration, steel fibers in UHPC are short, discontinuous, and well-embedded within an ultra-dense, low-permeability matrix. This matrix greatly limits chloride ion penetration and moisture ingress, which are the primary triggers of corrosion. As a result, most studies report that steel fibers in UHPC show minimal or no corrosion even after extended chloride exposure or accelerated aging tests [153, 156]. In fact, some researchers have observed that the dense hydration products surrounding fibers provide a passivating effect, delaying corrosion initiation. However, when fibers are cut or exposed at the surface during mixing or finishing, localized rust staining can occur, although this has little effect on mechanical performance. Therefore, while UHPC with steel fibers is not immune to corrosion, its high compactness and low porosity significantly mitigate the risk compared to conventional concrete.

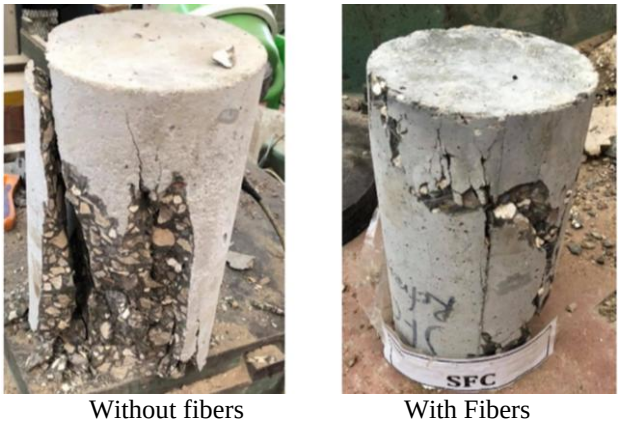

Without fibers With Fibers

Fig. 4. Concrete failure with and without fibers [122]

Table 2. Sample of prior research on the effect of fibers on the strength of UHPC

CONSTITUENT	SUMMARY	REFERENCES
STEEL FIBERS	The addition of steel fibers can considerably enhance split tensile	[45,116,117]
	Steel fibers are commonly utilized with volume fractions, ranging from 1% to 3%	[30]
	Concrete compressive strength improved by around 70% when adding 3% steel fibers.	[96]
	Although steel fibers have demonstrated a significant impact on tensile and flexural strength, their content has a limited effect on compressive strength	[118]
BASALT FIBERS	Hybrid of basalt fibers and polypropylene decreased compressive strength, but increased split tensile strength.	[119]
	The use of presoaked basalt fibers had no significant influence on the compressive strength.	[120]
SYNTHETIC FIBERS	Synthetic fibers can improve the split tensile and flexural strength	[121]
POLYPROPYLENE FIBERS	Polypropylene fibers exhibit a superior effect in enhancing the tensile and flexural strength of concrete compared to basalt fibers	[111]
	Utilizing polypropylene with 7.2% volume fraction significantly improved tensile and flexural strength	[111]

5. Durability properties

5.1. Freeze and Thaw

Freeze and thaw damage has emerged as a significant concern in the overpack concrete utilized in dry storage systems [9]. Evidence of freeze and thaw damage has been observed in various external concrete structures of nuclear power plants (Commission, 2019), including the outer surfaces of dry cask storage for spent nuclear fuel (SNF), the roofs of concrete storage modules at Three Mile Island Unit 2 (TMI-2), and the Millstone independent spent fuel storage installation during operation [9, 131]. In DCS's overpack, when freeze and thaw conditions are met, the degradation process would initiate at the outer surface of the overpack. The results of freeze and thaw action are often seen as random cracking, surface scaling, and joint degradation [9, 132, 133]. This degradation has a significant impact on the service life of DCS

The advancement of UHPC holds great promise in extending the service life of DCSS. The improved composition can reduce capillary porosity, allowing for greater resistance to freeze- thaw cycles [134–138]. Typically, concrete exposed to freeze and thaw cycles experiences material spalling and a reduction in relative dynamic modulus as a result of micro-cracking. However, multiple studies have demonstrated that UHPC is exceptionally resistant to freeze and thaw degradation. UHPC has been shown to have low mass loss even after 300 or 600 freeze and thaw cycles, with a high durability compared to conventional concrete [139–141]. Moreover, several studies showed no detectable damage after 800 freeze-thaw cycles [142].

A previous study [143] investigated the effects of using an air-entrained agent on four different concrete mixtures: normal concrete (NC), high-strength concrete (HSC), silica fume concrete (SFC), and fly ash concrete (FAC). As can be seen in **Fig. 5**, air entrained agents showed a considerable effect in reducing the surface scaling. Among all the concrete mixtures, HSC showed the lowest surface scaling. This can be attributed to the higher compressive strength obtained by HSC. On the other hand, the surface of silica fume concrete was more severely damaged than other concrete mixtures.

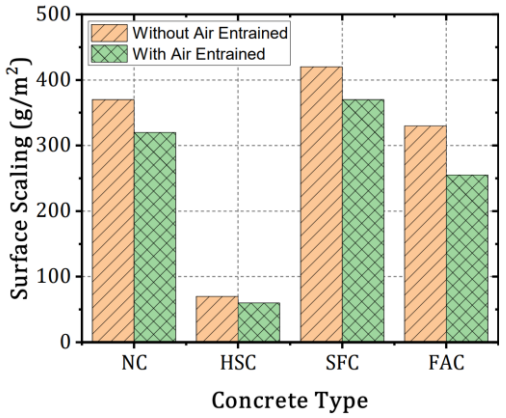

Fig. 5. Effect of air-entrained agent on the surface scaling of UHPC (Based on [143])

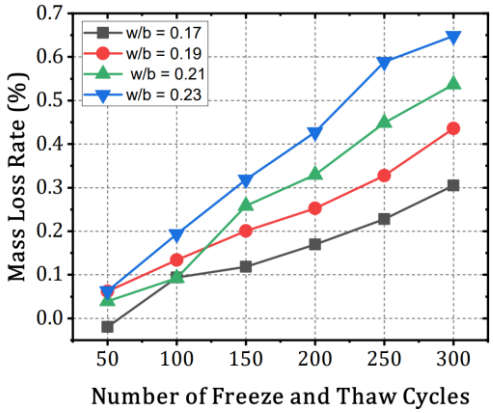

Fig. 6. Effect of w/b ratio on the mass loss rate of UHPC (Based on [144])

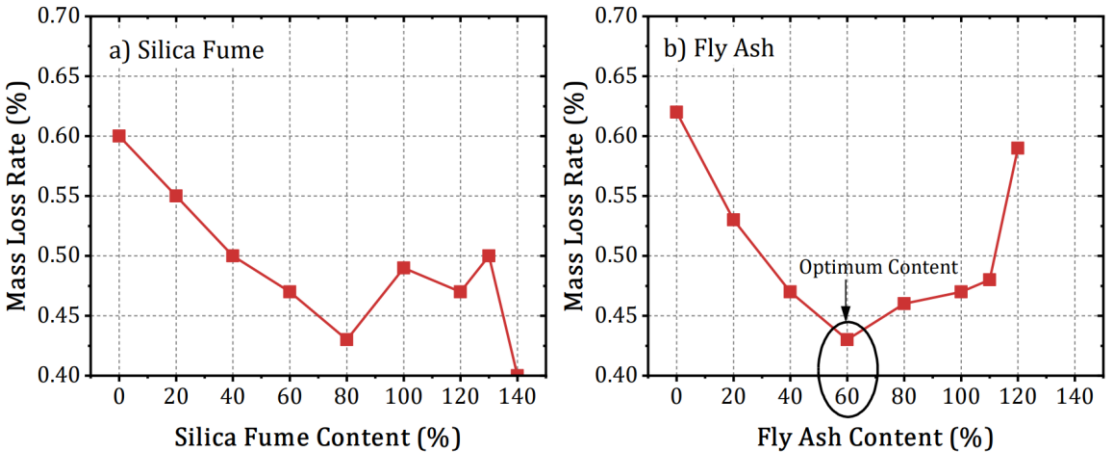

Fig. 7. Effect of SF and FA content on the mass loss rate of UHPC (Based on [144])

Another key factor influencing freeze-thaw resistance is the water-to-binder (w/b) ratio [144]. As can be seen in **Fig. 6**, it was observed that the mass loss rate of UHPC gradually increased with the increase in the number of freeze and thaw cycles. Additionally, the mass loss rate of UHPC demonstrated an increasing trend with higher w/b ratios. Freeze-thaw resistance is also affected by the content of SCMs [145, 146]. As illustrated in **Fig. 7**, the mass loss rate decreased as the content of SF and FA increased, until reaching a certain content, beyond which the loss rate began to rise.

5.2. Alkali-Aggregate Reaction (AAR)

Alkali-aggregate reaction (AAR) represents a credible risk in concrete exposed to any environment with available moisture, a concern reported in Dry Cask Storage (DCS) [9]. Recent operational experiences have highlighted ASR-induced concrete degradation in the Seabrook reactor enclosure. Despite passing all industry-standard ASR screening tests during construction, observations of ASR-induced degradation were made in August 2010 at the Seabrook plant [9].

In 1995, Ferraris [147] raised a question regarding the susceptibility of HPC to AAR. By this time, researchers have not reached an agreement on this matter, as factors be- yond the three primary ones, pore solution alkalinity, aggregate morphology, and water presence, also significantly influence ASR occurrence. These additional factors include aggregate gradation, water-to-cement ratio (w/c), and compressive strength. It has been found that air content is a crucial parameter, besides the three primary factors mentioned above, that can increase expansion in concretes affected by ASR. According to this study, even HPC may be susceptible to ASR if reactive aggregates are utilized.

Limited research has been conducted to investigate the resistance of HPC to AAR. However, some studies suggest that incorporating filling materials, such as SCMs, and employing methods to reduce permeability may enhance concrete's resistance to AAR [9]. For instance, the inclusion of FA decreases the $CaO{-}SiO_2$ ratio of Calcium-Silicate-Hydrate (C-S-H) gel, thereby enhancing its ability to retain alkalis. Additionally, the incorporation of alumina helps to reduce ASR by allowing the formation of calcium aluminum silicate hydrate (C- A-S-H). This compound possesses distinct properties compared to the C-S-H and enhances the binding of alkali ions from pore solutions, thereby preventing the continual recycling of these ions and the formation of the swelling complex [148, 149].

Recent research [150] revealed that concrete containing nanoparticles showed a reduced expansion and higher sonic velocity compared to plain concrete. This suggests that $nano-SiO_2$ and $nano-Fe_2O_3$ can effectively mitigate ASR damage, with optimal contents of 2% and 1% respectively. The common mechanisms by which $nano-SiO_2$ and $nano-Fe_2O_3$ mitigate ASR include their ultra-microsize, high activity, high-specific surface area, and surface hydrophilicity, allowing water consumption and hydration product occupation to reduce porosity. Additionally, $nano-SiO_2$ exhibits pozzolanic activity, consuming released CH during hydration, while $nano{-}Fe_2O_3$ has intense absorbability, forming block structures among hydration products. Consequently, concrete containing $nano{-}SiO_2$ or $nano{-}Fe_2O_3$ demonstrates a more compact microstructure and lower Ca^{2+} concentration in pore solution.

5.3. Corrosion

Corrosion of steel bars in a chlorine salt environment greatly affects the bearing capacity and service life of concrete structures [151]. Reinforcement corrosion has been identified as a major problem in DCS's overpack [9]. Both chloride ion penetration and reinforcement corrosion are closely related to concrete porosity [152]. Therefore, the improved composition of UHPC can effectively reduce corrosion probability.

Previous research has shown that UHPC is very resistant to chloride ion penetration. Mosavinejad et al. [153] proposed that adding polyvinyl alcohol fibers might effectively improve UHPC's resistance to chloride ion penetration by increasing electrical resistivity. Dieb et al. [154] found that increasing the steel fiber volume fraction from 0.08% to 0.52% resulted in greater chloride permeability in UHPC.

Chen et al. [155] studied various types of fiber-reinforced concrete to determine chloride penetration resistance. The results showed that a low volume fraction of microfibers improved concrete's resistance to chloride penetration, whereas a higher volume fraction in- creased chloride ion diffusion. The ideal microfibre volume fraction was determined to be less than 0.1%. However, Abbas et al. [156] claimed that the length and content of steel fibers had no detectable effect on the chloride

ion permeability of UHPC

5.4. Radiation

Researchers in concrete technology have investigated the possibility of employing specific concrete kinds to reduce or eliminate radiation transmission through structural parts. This focus has led to the development of radiation shielding concrete (RSC), which offers reliable protection against gamma rays and high-energy gamma-rays [157]. RSC, a composite concrete composition, may be designed to withstand both neutron and gamma radiation [158, 159]. However, standard radiation shielding materials such as lead have limitations, directing research into new materials such as heavyweight aggregate, pozzolanic additives, and fibers to improve RSC efficiency. Concrete's ability to shield against radiation is determined by factors such as mass density of the material of the protective material (which depends mainly on the aggregate), the atomic number of elements forming the aggregate and the radiation energy [158]. In general, increasing material density and atomic number enhance radiation attenuation, whereas higher radiation energy reduces the attenuation coefficient.

6. Advancing UHPC development

The utilization of advanced technologies, such as 3D printing in concrete production represents a transformative shift in construction methodology. By harnessing the precision and flexibility of 3D printing, concrete structures can be intricately designed and efficiently fabricated, offering unprecedented opportunities for architectural innovation and customization, **Fig. 8**. This technology enables the creation of complex geometries and intricate patterns that would be challenging or impossible to achieve with traditional construction methods [160]. Moreover, 3D printing facilitates enhanced material utilization and reduces construction waste, contributing to sustainability efforts within the industry. For example, eliminating conventional formwork, a major component of concrete casting, can reduce material use by up to 60% in optimized architectural applications like DFAB House (ETH Zurich). In reinforced concrete slabs, 3D-printed recesses enabled up to 40% volume savings and as much as 50% reduction in CO_2-equivalent emissions. Additionally, using advanced low-carbon printable mixtures (e.g., graphene-enhanced LC²) has been shown to reduce greenhouse gas emissions by approximately 31% compared to traditional printable concrete designs. As the capabilities of 3D printing continue to evolve, its integration into concrete production holds immense promise for streamlining construction processes, reducing costs, and pushing the boundaries of design possibilities in the built environment.

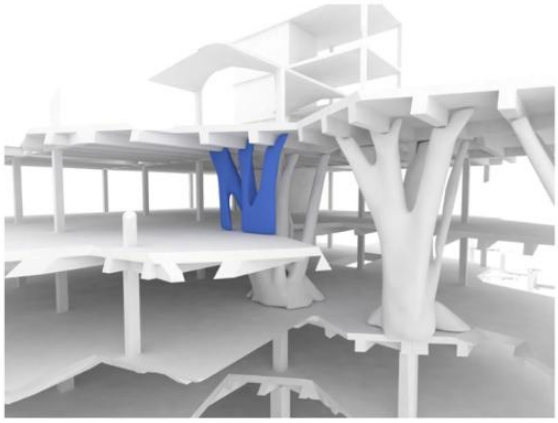

Fig. 8. Architectural context of 3D printing for complex geometries [160]

Fig. 9. 3D printed damping wall [160]

To facilitate concrete for additive manufacturing, achieving a balance between a low water-to-cement ratio and maintaining workability poses a significant challenge. Numerous researchers have endeavored to address this complexity by developing and testing various cementitious mixtures tailored for 3D printing applications. For instance, Zhang et al. [161] successfully formulated two cementitious materials using 3D printing, meeting crucial rheological requirements such as yield stresses and velocity.

Liu et al. [162] developed different mix designs by assessing rheological properties based on static and dynamic yield stresses to optimize flow and printing consistency. Tay et al. [163] investigated the bond strength be- tween printed layers and the impact of time intervals between successive prints, ensuring the mixture's pumpability while enhancing structural integrity. Moreover, Kazemian et al. [164] proposed four distinct cementitious formulations, incorporating high-range water-reducing admixtures alongside traditional components like cement, sand, and water, to address both printability and performance requirements.

In [165], an innovative automated 3D-printing concept was introduced, offering a versatile solution for fabricating various bridge components with UHPC, **Fig. 9**. This system particularly emphasizes the creation of UHPC shells, serving as stay-in-place formwork for bridge columns and beams [166]. Notably, the proposed 3D-printing system incorporates accelerated curing methods, leveraging heat curing techniques to expedite the curing process of the UHPC material.

7. Cost analysis

The goal of this research effort was to build cost-effective UHPC that is applicable to implementation in nuclear structures. One of the initial efforts to promote the use of UHPC in the United States was a project conducted in 2013 by Federal Highway Administration (FHWA) [63]. The objective was to create a non-proprietary, cost-effective UHPC with good durability qualities, a minimum compressive strength of 137.90 MPa, and a tensile strength of 4.96 MPa. Three geographical areas provided materials: (1) the New York, Connecticut, and New Jersey region; (2) the Upper Midwest, including the areas around Iowa, Minnesota, and Michigan; and (3) the Northwest, including the areas around Washington and Oregon. The cost of proprietary UHPC, including fiber and delivery, was over $2,000 per cubic yard at the time of the report (2013), which is roughly 20 times more than the standard.

FHWA [63] concentrated on the development of UHPC without fibers because the cost per cubic yard increased by around $470 when steel fibers were added to the mix. Cements (12 varieties), silica fumes (5 types), additional materials (13 types), high-range water reducers (8 types), HRWRs (8 types), and aggregates (10 variations) were among the locally accessible resources in the three zones. Four categories of aggregates were chosen: volcanic rock (VR), limestone (L), basalt (B), and quartz (Q). There are various US regions where Q can be ordered. Three people were chosen: L from the upper Midwest, VR from the Northwest, and B from the Northeast. Two distinct mixtures were made, one consisting solely of fine aggregates and the other of both fine and coarse particles. The ideal UHPC mixtures with just fine particles are displayed in **Table 3**. The material costs are displayed in the table's final row. The prices per cubic yard, in 2013 USD, varied from $472 to $652.

Table 3. UHPC mixtures with fine aggregates only and no fibers (FHWA 2013) [63]

Material/Topic	UHPC-1	UHPC-2	UHPC-3	UHPC-4
White Cement (lb./yd3)	1,311	1,268	1,256	1,248
Silica Fume (lb./yd3)	328	317	314	312
Fly Ash (lb./yd3)	318	308	305	303
HRWR (lb./yd3)	48	46	45	45
Fine Aggregates (lb./yd3)	1,966	1,903	1,884	1,871
Aggregated-to-Cement Ration (lb./yd3)	1.5	1.5	1.5	1.5
w/c ratio	0.23	0.24	0.23	0.23
Spread (in)	11.4	10.4	11.3	12.4
Average Compressive Strength-28 days (ksi)	26.9	24.1	23.5	29
Cost ($/yd3)	494	472	496	652

Montana Department of Transportation [167] was able to create and describe non- proprietary UHPC mix designs utilizing readily available local materials. When this project is finished, traditional UHPC qualities can be used in concrete at a lower cost (Montana DOT 2017) [167]. The Montana Department of Transportation plans to include this new non-proprietary UHPC mix design into their building practices—such as field-cast connections between precast concrete deck panels and between the flanges of adjacent girders—once this material is more widely available. Mixes that met design goals were found to be less than $1,000/yd^3 using materials found within Montana. The material and

labor cost for the Montana UHPC (MT-UHPC) used in this bridge construction was found to be $4,560 per cubic yard, as outlined in **Table 4**, and non-proprietary UHPC, as **Table 5** illustrates.

Table 4. Cost of MT-UHPC per cubic yard

Item	Cost ($/yd3)
Cement	237
Silica Fume	174
Fly Ash	204
HRWR	68
Steel Fibers	790
Sand	77
Material Subtotal	1,550
Mixing	850
Total Materials Cost	2,400
Grinding	370
Placement	1,790
Total	4,560

The interface bond strength between UHPC and precast concrete was tested. Shokrgozar examined interface bond using 8 ksi (55.16 MPa), 10 ksi (68.95 MPa), and 12 ksi (82.74 MPa) concrete, in contrast to Haber et al.'s (FHWA 2018) experiments that used 6 ksi (41.37 MPa) precast concrete. All interface failures in this investigation happened at the interface where precast concrete and UHPC met, and the strength rose as precast compressive strength rose.

Table 5. Material comparison (Shokrgozar 2023) [169]

	Non-Proprietary	Proprietary UHPC
Flow Table Test, (in)	10	10
Compressive Strength, (ksi)	18.1	20.1
Tensile Strength, (ksi)	2.8	2.9
Average Interface Bond Strength		
Precast Concrete with 8 ksi, 10 ksi, and 12 ksi, psi	651	696
Shrinkage (336 days), Micro-strain	290	410
Modulus of Elasticity	6,950	7,370
Poisson' Ratio	0.19	0.2
Bridge Deck Connection Ultimate Moment, (k-ft)	61	67
Material Cost ($/yd3)	$350	$2,000

El-Tawil et al. [168] at the University of Michigan developed a non-proprietary UHPC that worked well in the lab as part of their initial project phase. A Michigan bridge restoration project used one of the mixtures created during this study. The average 28-day compressive strength and tensile strength of the field UHPC mix were 148.24 MPa and 8.27 MPa, respectively. The material cost per cubic yard, as recorded, was $890 in 2017 USD.

Ali Shokrgozar (2023) [169] at Idaho State University created a non-proprietary UHPC utilizing locally accessible materials in Idaho and contrasted its characteristics with a widely used proprietary UHPC. Fine aggregates, Type I/II Portland cement, silica fume, Type F fly ash, HRWR, and steel fibers were the materials utilized. The steel fibers came from within the country. The development of non-proprietary UHPC at Idaho State University, with a focus on closing connections for bridge deck-level precast components, is covered in detail in the paper's conclusion. Compared to proprietary UHPC, which costs more than $2,000 per cubic yard, the estimated material cost of $350 per cubic yard is substantially lower. Compressive strength, splitting tensile strength, four-point flexural strength, shrinkage, modulus of elasticity, and Poisson's ratio were all tested experimentally. To assess the closing pour connection's moment capacity, extensive bridge deck connection tests were also carried out. The findings show that non-proprietary UHPC behaves in a manner that is strikingly comparable to proprietary UHPC.

8 Conclusions

The findings of this study reaffirm the substantial benefits of incorporating supplementary cementitious materials into ultra-high-performance concrete. The use of silica fume, fly ash, and metakaolin not only enhances the mechanical properties of UHPC but also improves its durability, sustainability, and overall performance in demanding structural applications. Silica fume, due to its high pozzolanic reactivity, plays a crucial role in refining microstructure and increasing compressive strength. Fly ash, when used in appropriate proportions, enhances long-term strength development while improving workability and reducing permeability. Metakaolin, recognized for its ability to refine pore structure, further contributes to enhanced durability and mechanical performance. The synergistic effect of these SCMs enables the development of UHPC with optimized properties, catering to the increasing demand for high-strength, long-lasting construction materials.

Despite these advancements, further research is warranted to explore the combined effects of multiple SCMs and their influence on large-scale structural performance. Additionally, studies on the economic feasibility, life-cycle assessment, and environmental impact of SCM-integrated UHPC are essential to maximize its adoption in the construction industry. The continuous innovation in UHPC formulation and material technology will play a pivotal role in shaping the future of sustainable infrastructure, paving the way for more resilient, efficient, and environmentally responsible construction solutions.

Acknowledgement

Acknowledgements and Reference heading should be left justified, bold, with the first letter capitalized but have no numbers. Text below continues as normal.

Funding Statement

This study has been funded by the Center for Advanced Energy Studies (CAES), Idaho National Laboratory.

CRediT authorship contribution statement

Mohamed T. Elshazli, Ahmed Ibrahim: Conceptualization, Investigation, Formal analysis, Writing – original draft, Writing – review & editing. **Elmar Eidelpes, Gabriel O Ilevbare**: Conceptualization, Supervision, Writing – review & editing.

Conflicts of Interest

The authors declare that they have no conflicts of interest to report regarding the present study.

Data Availability Statement

Some or all data, models, or codes that support the findings of this study are available from the corresponding author upon reasonable request.

References

[1] Vitkova M, Gorinov I, Dacheva D. Safety criteria for wet and dry spent fuel storage. In: Proceedings of the International Conference on WWER Fuel Performance, Modelling and Experimental Support, Albena, Bulgaria, 19–23 September 2005. U.S. Department of Energy OSTI 2005. Available at: https://www.osti. g ov/etdeweb/biblio/20796269

[2] Ewing RC. Long-term storage of spent nuclear fuel. Nature Materials 2015; 14(3): 252–257. https://doi.org/ 10.1038/nmat4226.

[3] Nuclear Waste Technical Review Board. Evaluation of the technical basis for extended dry storage and transportation of used nuclear fuel: executive summary. U.S. Nuclear Waste Technical Review Board; 2010. Available at. https://www.govinfo.gov/app/details/GOVPUB-Y3_N88_2-PURL-gpo24144.

[4] Bare WC, Ebner MA, Torgerson LD. Dry cask storage characterization project-Phase 1: CASTOR V/21 cask opening and examination (No. INEEL/EXT-01-00183). Idaho National Lab., Idaho Falls, ID (United States) 2001. https://doi.org/10.2172/911204.

[5] Macfarlane A. Interim storage of spent fuel in the United States. Annual Review of Energy and the

Environment 2001; 26(1): 201–235. https://doi.org/10.1146/annurev.energy.26.1.201.
[6] U.S. Government Accountability Office. Spent Nuclear Fuel: Accumulating Quantities at Commercial Reactors Present Storage and Other Challenges (GAO-12-797). Washington, D.C. U.S. Government Accountability Office 2012. Available at: https://www.gao.gov/products/gao-12-797.
[7] Haire MJ, Swaney P. Cask size and weight reduction through the use of depleted uranium dioxide (DUO_2)–steel cermet material. Waste Management 2005. https://doi.org/10.15407/jnpae2007.01.089.
[8] Wimmer H, Skrzyppek J, Köbl M. CASTOR® and CONSTOR®: A well-established system for the dry storage of spent fuel and high-level waste. VGB Power Tech 2015; 95(5): 52–57. (company/technical report available at GNS materials describing this system)
[9] Elshazli MT, Ibrahim A, Eidelpes E, Ilevbare GO. Degradation mechanisms in overpack concrete of spent nuclear fuel dry storage systems: A review. Nuclear Engineering and Design 2023; 414: 112632. https://doi.org/10.1016/j.nucengdes.2023.112632.
[10] Oberson G, Dunn D, Hiser M, Torres R, Tripathi B, Wise J, Wong E, Pan Y, He X, Chowdhury A, et al. Identification of potential degradation phenomena for spent fuel dry cask storage systems. U.S. Nuclear Regulatory Commission; 2015. (official NRC report accessible from NRC publications)
[11] Dong S, Gu J, Ouyang X, Jang S-H, Han B. Enhancing mechanical properties, durability and multifunctionality of concrete structures via using ultra-high-performance concrete layer: A review. Composites Part B: Engineering 2025; 112329. https://doi.org/10.1016/j.compositesb.2025.112329. Source: Elsevier – https://www.sciencedirect.com/science/article/pii/S135983682500329X
[12] Almakrab A, Elshazli MT, Ibrahim A, Khalifa YA. Assessment of various mitigation strategies of alkali-silica reactions in concrete using accelerated mortar test. Materials 2024; 17(20): 5124. https://doi.org/10. 3390/ma17205124.
[13] Semmana O, Rihan MAM, Barrie ZM, Daniel C, Abdalla TA. A systematic review of the strength, durability, and microstructure properties of concrete incorporating glass powder. Engineering Reports 2025; 7(1): e70002. https://doi.org/10.1002/eng2.70002.
[14] De la Varga I, Graybeal BA. Dimensional stability of grout-type materials used as connections between prefabricated concrete elements. Journal of Materials in Civil Engineering 2015; 27(9): 04014246. https://doi.org/10.1061/(ASCE)MT.1943-5533.0001212.
[15] Wille K, Naaman AE, Parra-Montesinos GJ. Ultra-high-performance concrete with compressive strength exceeding 150 MPa (22 ksi): A simpler way. ACI Materials Journal 2011; 108(1). https://doi.org/10. 14359/51664215.
[16] Habel K, Viviani M, Denarié E, Brühwiler E. Development of the mechanical properties of an ultra-high performance fiber reinforced concrete (UHPCFRC). Cement and Concrete Research 2006; 36(7): 1362–1370. https://doi.org/10.1016/j.cemconres.2006.03.009.
[17] Meng Q, Wu C, Li J, Liu Z, Wu P, Yang Y, Wang Z. Steel/basalt rebar reinforced ultra-high performance concrete components against methane-air explosion loads. Composites Part B: Engineering 2020; 198: 108215. https://doi.org/10.1016/j.compositesb.2020.108215.
[18] Li P, Sluijsmans MJ, Brouwers H, Yu Q. Functionally graded ultra-high performance cementitious composite with enhanced impact properties. Composites Part B: Engineering 2020; 183: 107680. https://doi.org/10. 1016/j.compositesb.2019.107680.
[19] Richard P, Cheyrezy M. Composition of reactive powder concretes. Cement and Concrete Research 1995; 25(7): 1501–1511. https://doi.org/10.1016/0008-8846(95)00144-2.
[20] Caldarone MA. High-Strength Concrete: A Practical Guide. Boca Raton, FL: CRC Press; 2014. ISBN 978-0415404326. Source: https://www.routledge.com/High-Strength-Concrete-A-Practical-Guide/Caldar one/p/book/9780415404326
[21] Azmee NM, Shafiq N. Ultra-high-performance concrete: From fundamental to applications. Case Studies in Construction Materials 2018; 9: e00197. https://doi.org/10.1016/j.cscm.2018.e00197.
[22] Camacho Torregrosa EE. Dosage optimization and bolted connections for UHPCFRC ties. PhD Thesis. Universitat Politècnica de València; 2014. Source: UPV Repository –https://riunet.upv.es/handle/10251/38625
[23] Abdo A, Elshazli MT, Alashker Y, Ahmed S. Improving flexural response of rubberized RC beams with multi-dimensional sustainable approaches. Construction and Building Materials 2024; 449: 138400. https://doi.org/10.1016/j.conbuildmat.2024.138400.
[24] Du J, Meng W, Khayat KH, Bao Y, Guo P, Lyu Z, Abu-Obeidah A, Nassif H, Wang H. New development of ultra-high-performance concrete (UHPC). Composites Part B: Engineering 2021; 224: 109220. https://doi.org/10.1016/j.compositesb.2021.109220.
[25] Stovall T, De Larrard F, Buil M. Linear packing density model of grain mixtures. Powder Technology 1986; 48(1): 1–12. https://doi.org/10.1016/0032-5910(86)80058-4.
[26] De Larrard F, Sedran T. Mixture-proportioning of high-performance concrete. Cement and Concrete Research 2002; 32(11): 1699–1704. https://doi.org/10.1016/S0008-8846(02)00861-X.

[27] Fennis S, Walraven J, Den Uijl J. Compaction-interaction packing model: regarding the effect of fillers in concrete mixture design. Materials and Structures 2013; 46: 463–478. https://doi.org/10.1617/s11527-013-0014-8.
[28] Fuller WB, Thompson SE. The laws of proportioning concrete. Transactions of the American Society of Civil Engineers 1907; 59(2): 67–143. https://doi.org/10.1061/TACEAT.0001979.
[29] Andreasen A. Ueber die Beziehung zwischen Kornabstufung und Zwischenraum in Produkten aus losen Körnern. Kolloid-Zeitschrift 1930; 50: 217–228. https://doi.org/10.1007/BF01422986.
[30] Funk JE, Dinger DR. Predictive process control of crowded particulate suspensions: Applied to ceramic manufacturing. New York: Springer 2013. https://doi.org/10.1007/978-1-4615-3118-0.
[31] Mehdipour I, Khayat KH. Understanding the role of particle packing characteristics in rheo-physical properties of cementitious suspensions: A literature review. Construction and Building Materials 2018; 161: 340–353. https://doi.org/10.1016/j.conbuildmat.2017.11.147.
[32] Hunger M. An integral design concept for ecological self-compacting concrete. PhD Thesis. Eindhoven University of Technology 2010; ISBN 978-90-6814-628-8. Source: TU/e Repository –https://pure.tue. nl/ws/portalfiles/portal/4697893/643981.pdf
[33] Yu R, Spiesz P, Brouwers H. Development of an eco-friendly ultra-high-performance concrete with efficient cement and mineral admixtures uses. Cement and Concrete Composites 2015; 55: 383–394. https://doi.or g/10.1016/j.cemconcomp.2014.09.024.
[34] Yu R, Spiesz P, Brouwers H. Mix design and properties assessment of ultra-high performance fibre reinforced concrete (UHPCFRC). Cement and Concrete Research 2014; 56: 29–39. https://doi.org/10.1016/j.cemconres.2013.11.002.
[35] Li L, Kwan AKH. Packing density of concrete mix under dry and wet conditions. Powder Technology 2014; 253: 514–521. https://doi.org/10.1016/j.powtec.2013.12.020.
[36] Iveson SM, Wauters PA, Forrest S, Litster JD, Meesters GMH, Scarlett B. Growth regime map for liquid-bound granules: Further development and experimental validation. Powder Technology 2001; 117(1–2): 83–97. https://doi.org/10.1016/S0032-5910(01)00317-5.
[37] Wang X, Yu R, Song Q, Shui Z, Liu Z, Wu S, Hou D. Optimized design of ultra-high-performance concrete with a high wet packing density. Cement and Concrete Research 2019; 126: 105921. https://doi.org/10. 1016/j.cemconres.2019.105921.
[38] Meng W, Valipour M, Khayat KH. Optimization and performance of cost-effective ultra-high-performance concrete. Materials and Structures 2017; 50: 1–16. https://doi.org/10.1617/s11527-016-0896-3.
[39] Shi C, Wu Z, Xiao J, Wang D, Huang Z, Fang Z. A review on ultra-high performance concrete: Part I. Raw materials and mixture design. Construction and Building Materials 2015; 101: 741–751. https://doi.org/10.1016/j.conbuildmat.2015.10.088.
[40] Lin Y, Yan J, Wang Z, Fan F, Zou C. Effect of silica fume on fluidity of UHPC: Experiments, influence mechanism, and evaluation methods. Construction and Building Materials 2019; 210: 451–460. https://doi.org/10.1016/j.conbuildmat.2019.03.162.
[41] Wu Z, Khayat KH, Shi C. Changes in rheology and mechanical properties of ultra-high-performance concrete with silica fume content. Cement and Concrete Research 2019; 123: 105786. https://doi.org/10.1016/j. cemconres.2019.105786.
[42] Xi J, Liu J, Yang K, Zhang S, Han F, Sha J, Zheng X. Role of silica fume on hydration and strength development of ultra-high-performance concrete. Construction and Building Materials 2022; 338: 127600. https://doi.org/10.1016/j.conbuildmat.2022.127600.
[43] Soliman NA, Tagnit-Hamou A. Using glass sand as an alternative for quartz sand in UHPC. Construction and Building Materials 2017; 145: 243–252. https://doi.org/10.1016/j.conbuildmat.2017.03.187.
[44] Zhang H, Ji T, He B, He L. Performance of UHPC with cement partially replaced by ground granite powder under different curing conditions. Construction and Building Materials 2019; 213:469–482. https://doi. org/10.1016/j.conbuildmat.2019.04.058.
[45] Xiong X, Wu M, Shen W, Li J, Zhao D, Li P, Wu J. Performance and microstructure of UHPC with silica fume replaced by inert mineral powders. Construction and Building Materials 2022; 327: 126996. https://doi.org/10.1016/j.conbuildmat.2022.126996.
[46] Li P, Yu Q, Brouwers H. Effect of PCE-type superplasticizer on early-age behavior of UHPC. Construction and Building Materials 2017; 153: 740–750. https://doi.org/10.1016/j.conbuildmat.2017.07.145.
[47] Tue NV, Ma J, Orgass M, et al. Influence of addition method of superplasticizer on the properties of fresh UHPC. In: Proceedings of the 2nd International Symposium on Ultra-High-Performance Concrete, Kassel, Germany 2008: 93–100. Source: Kassel University Press.
[48] Schröfl C, Gruber M, Plank J. Preferential adsorption of polycarboxylate superplasticizers on cement and silica fume in UHPC. Cement and Concrete Research 2012; 42(11): 1401–1408. https://doi.org/10.1016/j.cemconres.2012.08.013.
[49] Mendonca F, Hu J. Impact of chemical admixtures on time-dependent workability and rheological properties

of UHPC. ACI Materials Journal 2021; 118(6). https://doi.org/10.14359/51734151.
[50] Plank J, Sakai E, Miao C, Yu C, Hong J. Chemical admixtures—chemistry, applications and their impact on concrete microstructure and durability. Cement and Concrete Research 2015; 78: 81–99. https://doi.org/10.1016/j.cemconres.2015.05.016.
[51] Yoo D-Y, Oh T, Banthia N. Nanomaterials in UHPC – a review. Cement and Concrete Composites 2022; 104730. https://doi.org/10.1016/j.cemconcomp.2022.104730.
[52] Liu C, He X, Deng X, Wu Y, Zheng Z, Liu J, Hui D. Application of nanomaterials in UHPC: A review. Nanotechnology Reviews 2020; 9(1): 1427–1444. https://doi.org/10.1515/ntrev-2020-0107.
[53] Luo Z, Zhi T, Liu X, Yin K, Pan H, Feng H, Song Y, Su Y. Effects of nanomaterials on early performance of UHPC: C–S–H seeds and nano-silica. Cement and Concrete Composites 2023; 142: 105211. https://doi.org/10.1016/j.cemconcomp.2023.105211.
[54] Wu Z, Shi C, Khayat KH, Wan S. Effects of different nanomaterials on hardening and performance of UHSC. Cement and Concrete Composites 2016; 70: 24–34. https://doi.org/10.1016/j.cemconcomp.2016.03.003.
[55] Zhang P, Wang L, Wei H, Wang J. A critical review on effect of nanomaterials on workability and mechanical properties of high-performance concrete. Advances in Civil Engineering 2021; 2021: 8827124. https://doi.org/10.1155/2021/8827124.
[56] Meng W, Khayat KH. Enhancing UHPC performance using carbon nanomaterials. In: International Interactive Symposium on Ultra-High Performance Concrete, Vol. 2. Iowa State University Digital Press; 2019. https://doi.org/10.21838/uhpc.9649.
[57] Graybeal BA, Hartmann JL. Strength and durability of UHPC. In: Concrete Bridge Conference; 2003.
[58] Graybeal BA, et al. Material property characterization of ultra-high-performance concrete. FHWA-HRT-06-103. Washington, DC: Federal Highway Administration; 2006.
[59] Talebinejad I, Bassam SA, Iranmanesh A, Shekarchizadeh M. Optimizing mix proportions of reactive powder concrete with strengths of 200–350 MPa. In: Proceedings of the International Symposium on UHPC, Kassel, Germany 2004; 133–141.
[60] Strunge T, Deuse T. Special cements for ultra-high-performance concrete. In: Proceedings of the Second International Symposium on UHPC, Kassel, Germany 2008; 61–68.
[61] Alsalman A, Dang CN, Hale WM. Development of UHPC with locally available materials. Construction and Building Materials 2017; 133: 135–145. https://doi.org/10.1016/j.conbuildmat.2016.12.040.
[62] Budelmann H, Ewert J. Mechanical properties of UHPC at early age. In: Ultra-High-Performance Concrete and Nanotechnology in Construction – HIPERMAT 2012. Kassel University Press 2012; 301.
[63] Graybeal BA, et al. Development of non-proprietary UHPC for use in the highway bridge sector. FHWA Tech Brief 2013.
[64] Ahmed S, Elshazli MT, Zaghlal M, Alashker Y, Abdo A. Improving shear behavior of rubberized concrete beams through sustainable integration of waste tire steel fibers and treated rubber. Journal of Building Engineering 2024; 96: 110649. https://doi.org/10.1016/j.jobe.2024.110649.
[65] Dushimimana A, Niyonsenga AA, Nzamurambaho F. A review on strength development of high-performance concrete. Construction and Building Materials 2021; 307: 124865. https://doi.org/10.1016/j.conbuildmat. 2021.124865.
[66] Chan Y-W, Chu S-H. Effect of silica fume on steel fiber bond characteristics in reactive powder concrete. Cement and Concrete Research 2004; 34(7): 1167–1172. https://doi.org/10.1016/j.cemconres.2003.12.023.
[67] Dembovska L, Bajare D, Pundiene I, Vitola L. Effect of pozzolanic additives on strength development of HPC. Procedia Engineering 2017; 172: 202–210. https://doi.org/10.1016/j.proeng.2017.02.050.
[68] Wong HS, Razak HA. Efficiency of calcined kaolin and silica fume as cement replacement. Cement and Concrete Research 2005; 35(4): 696–702. https://doi.org/10.1016/j.cemconres.2004.05.051.
[69] Behnood A, Ziari H. Effect of silica fume addition on high-strength concrete after exposure to high temperatures. Cement and Concrete Composites 2008; 30(2): 106–112. https://doi.org/10.1016/j.cemconcomp.2007.06.003.
[70] Yazıcı H, Yiğiter H, Karabulut AŞ, Baradan B. Utilization of fly ash and GGBFS as alternative silica source in RPC. Fuel 2008; 87(12): 2401–2407. https://doi.org/10.1016/j.fuel.2008.03.005.
[71] Yazıcı H, Yardımcı MY, Aydın S, Karabulut AŞ. Mechanical properties of RPC under different curing regimes. Construction and Building Materials 2009; 23(3): 1223–1231. https://doi.org/10.1016/j.conbuildmat.2008.08.003.
[72] Peng Y, Hu S, Ding Q. Preparation of RPC using fly ash and steel slag powder. Journal of Wuhan University of Technology – Materials Science Edition 2010; 25: 349–354. https://doi.org/10.1007/s11595-010-2349-0.
[73] Chore H, Joshi M. Strength evaluation of concrete with fly ash and GGBFS. Advances in Concrete Construction 2015; 3(3): 223. https://doi.org/10.12989/acc.2015.3.3.223.
[74] Phul AA, Memon MJ, Shah SNR, Sandhu AR. GGBS and fly ash effects on compressive strength. Civil Engineering Journal 2019; 5(4): 913–921. https://doi.org/10.28991/cej-2019-03091299.
[75] Pera J, Bonnin E. Inertization of toxic metals in metakaolin-blended cements. American Ceramic Society

Technical Report 1996.
[76] Pera J, Bonnin E, Chabannet M. Immobilization of wastes by metakaolin-blended cements. ACI Special Publication 1998; 178: 997–1006.
[77] Barger GS, Lukkarila MR, Martin DL, Lane SB, Hansen ER, Ross MW, Thompson JL. Evaluation of blended cement with calcined clay natural pozzolans for HPC. In: International Purdue Conference on Concrete Pavement Design and Materials for High Performance 1997. https://doi.org/10.33593/iccp.v6i1.678.
[78] Shen P, Lu L, Chen W, Wang F, Hu S. Efficiency of metakaolin in steam-cured high-strength concrete. Construction and Building Materials 2017; 152: 357–366. https://doi.org/10.1016/j.conbuildmat.2017.07.006.
[79] Barbhuiya S, Chow P, Memon S. Microstructure and nanomechanical properties of concrete with metakaolin. Construction and Building Materials 2015; 95: 696–702. https://doi.org/10.1016/j.conbuildmat.2015.07.101.
[80] Güneyisi E, Gesoğlu M, Özbay E. Strength and drying shrinkage of SCC with blended mineral admixtures. Construction and Building Materials 2010; 24(10): 1878–1887. https://doi.org/10.1016/j.conbuildm at.2010.04.015.
[81] Hussain F, Kaur I, Hussain A. Influence of GGBFS on concrete properties. Materials Today: Proceedings 2020; 32: 997–1004. https://doi.org/10.1016/j.matpr.2020.07.410.
[82] Kumar VP, Gunasekaran K, Shyamala T. Coconut shell concrete with partial replacement by GGBS. Journal of Building Engineering 2019; 26: 100830. https://doi.org/10.1016/j.jobe.2019.100830.
[83] Xie J, Chen W, Wang J, Fang C, Zhang B, Liu F. Coupling effects of recycled aggregate and GGBS/metakaolin on geopolymer concrete. Construction and Building Materials 2019; 226: 345–359. https://doi.org/10.1016/j.conbuildmat.2019.07.311.
[84] Dadsetan S, Bai J. Mechanical and microstructural properties of SCC blended with metakaolin, GGBFS, and fly ash. Construction and Building Materials 2017; 146: 658–667. https://doi.org/10.1016/j.conb uildmat. 2017.04.158.
[85] Van VT, Ludwig H-M. Proportioning optimization of UHPC containing rice husk ash and ground granulated blast-furnace slag. In: Proceedings of the 3rd International Symposium on UHPC and Nanotechnology for High Performance Construction Materials (Hipermat 2012), Kassel, Germany 2012; 197–205. Source record: https://www.concrete.org/publications/internationalconcreteabstractsportal.aspx?ID=51742043&m=details.
[86] Bentur A, Goldman A, Cohen MD. The contribution of the transition zone to the strength of high-quality silica fume concretes. MRS Online Proceedings Library (OPL) 1987; 114: 97. https://doi.org/10.1557/PROC-114-97.
[87] Mazloom M, Ramezanianpour AA, Brooks JJ. Effect of silica fume on mechanical properties of high-strength concrete. Cement and Concrete Composites 2004; 26(4): 347–357. https://doi.org/10.1016/S0958-9465(03)00017-9.
[88] Hooton RD. Influence of silica fume replacement of cement on physical properties and resistance to sulfate attack, freezing and thawing, and alkali-silica reactivity. ACI Materials Journal 1993; 90(2): 143–151. https://doi.org/10.14359/4009.
[89] Tanyildizi H, Coskun A. Performance of lightweight concrete with silica fume after high temperature. Construction and Building Materials 2008; 22(10): 2124–2129. https://doi.org/10.1016/j.conbuildmat. 2007.07.017.
[90] Bhanja S, Sengupta B. Influence of silica fume on the tensile strength of concrete. Cement and Concrete Research 2005; 35(4): 743–747. https://doi.org/10.1016/j.cemconres.2004.05.024.
[91] Kayali O. Fly ash lightweight aggregates in high performance concrete. Construction and Building Materials 2008; 22(12): 2393–2399. https://doi.org/10.1016/j.conbuildmat.2007.09.001.
[92] Sabir BB, Wild S, Bai J. Metakaolin and calcined clays as pozzolans for concrete: A review. Cement and Concrete Composites 2001; 23(6): 441–454. https://doi.org/10.1016/S0958-9465(00)00092-5.
[93] Wild S, Khatib JM, Jones A. Relative strength, pozzolanic activity and cement hydration in superplasticised metakaolin concrete. Cement and Concrete Research 1996; 26(10): 1537–1544. https://doi.org/10.1016/0008-8846(96)00148-2.
[94] El-Diadamony H, Amer AA, Sokkary TM, El-Hoseny S. Hydration and characteristics of metakaolin pozzolanic cement pastes. HBRC Journal 2018; 14(2): 150–158. https://doi.org/10.1016/j.hbrcj.2015.05.005.
[95] Tafraoui A, Escadeillas G, Lebaili S, Vidal T. Metakaolin in the formulation of UHPC. Construction and Building Materials 2009; 23(2): 669–674. https://doi.org/10.1016/j.conbuildmat.2008.02.018.
[96] Rovnaník P. Effect of curing temperature on the development of hard structure of metakaolin-based geopolymer. Construction and Building Materials 2010; 24(7): 1176–1183. https://doi.org/10.1016/j. conbuildmat.2009.12.023.
[97] Xu S, Yuan P, Liu J, Pan Z, Liu Z, Su Y, Li J, Wu C. Development and preliminary mix design of ultra-high-performance concrete based on geopolymer. Construction and Building Materials 2021; 308: 125110. https://doi.org/10.1016/j.conbuildmat.2021.125110.
[98] Tran TM, Trinh HT, Nguyen D, Tao Q, Mali S, Pham TM. Development of sustainable ultra-high-

performance concrete containing ground granulated blast furnace slag and glass powder: Mix design investigation. Construction and Building Materials 2023; 397: 132358. https://doi.org/10.1016/j.conbuildmat.2023.132358.

[99] Yazıcı H, Yardımcı MY, Yiğiter H, Aydın S, Türkel S. Mechanical properties of reactive powder concrete containing high volumes of ground granulated blast furnace slag. Cement and Concrete Composites 2010; 32(8): 639–648. https://doi.org/10.1016/j.cemconcomp.2010.07.005.

[100] Wetzel A, Middendorf B. Influence of silica fume on properties of fresh and hardened ultra-high-performance concrete based on alkali-activated slag. Cement and Concrete Composites 2019; 100: 53–59. https://doi.org/10.1016/j.cemconcomp.2019.03.023.

[101] Seleem HEDH, Rashad AM, El-Sabbagh BA. Durability and strength evaluation of high-performance concrete in marine structures. Construction and Building Materials 2010; 24(6): 878–884. https://doi.o rg/10.1016/j.conbuildmat.2010.01.013.

[102] Lim SN, Wee TH. Autogenous shrinkage of ground-granulated blast-furnace slag concrete. ACI Materials Journal 2000; 97(5): 587–593. Source record: https://www.concrete.org/publications/internationalconcreteabstractsportal.aspx?ID=9291&m=details.

[103] Tan K, Zhu J. Influences of steam and autoclave curing on the strength and chloride permeability of high strength concrete. Materials and Structures 2017; 50: 56 (Article). https://doi.org/10.1617/s11527-016-0913-6.

[104] Zhutovsky S, Kovler K, Bentur A. Influence of cement paste matrix properties on the autogenous curing of high-performance concrete. Cement and Concrete Composites 2004; 26(5): 499–507. https://doi.org/10. 101 6/S0958-9465(03)00082-9.

[105] Xu L, Wu F, Chi Y, Cheng P, Zeng Y, Chen Q. Effects of coarse aggregate and steel fibre contents on mechanical properties of high-performance concrete. Construction and Building Materials 2019; 206: 97–110. https://doi.org/10.1016/j.conbuildmat.2019.01.190.

[106] Suzuki M, Meddah MS, Sato R. Use of porous ceramic waste aggregates for internal curing of high-performance concrete. Cement and Concrete Research 2009; 39(5): 373–381. https://doi.org/10.1016/j.cemconres.2009.01.007.

[107] Jóźwiak-Niedźwiedzka D. Scaling resistance of high performance concretes containing a small portion of pre-wetted lightweight fine aggregate. Cement and Concrete Composites 2005; 27(6): 709–715. https://doi.org/10.1016/j.cemconcomp.2004.11.001.

[108] Jiang C, Yang Y, Wang Y, Zhou Y, Ma C. Autogenous shrinkage of high-performance concrete containing mineral admixtures under different curing temperatures. Construction and Building Materials 2014; 61: 260–269. https://doi.org/10.1016/j.conbuildmat.2014.03.023.

[109] Kadri E, Aggoun S, Kenai S, Kaci A, et al. The compressive strength of high-performance concrete and ultrahigh-performance concrete. Advances in Materials Science and Engineering 2012; 2012: 361857. https://doi.org/10.1155/2012/361857.

[110] Bharatkumar B, Narayanan R, Raghuprasad B, Ramachandramurthy D. Mix proportioning of high-performance concrete. Cement and Concrete Composites 2001; 23(1): 71–80. https://doi.org/10.1016/S0958-9465(00)00071-8.

[111] Golias M, Castro J, Weiss J. The influence of the initial moisture content of lightweight aggregate on internal curing. Construction and Building Materials 2012; 35: 52–62. https://doi.org/10.1016/j.conbuildmat.2012.02.074.

[112] Cusson D, Hoogeveen T. Internal curing of high-performance concrete with pre-soaked fine lightweight aggregate for prevention of autogenous shrinkage cracking. Cement and Concrete Research 2008; 38(6): 757–765. https://doi.org/10.1016/j.cemconres.2008.02.001.

[113] Tu T-Y, Chen Y-Y, Hwang C-L. Properties of high-performance concrete with recycled aggregates. Cement and Concrete Research 2006; 36(5): 943–950. https://doi.org/10.1016/j.cemconres.2005.11.022.

[114] Kou S-C, Poon C-S. Effect of the quality of parent concrete on the properties of high-performance recycled aggregate concrete. Construction and Building Materials 2015; 77: 501–508. https://doi.org/10.1016/j.conbuildmat.2014.12.035.

[115] Yang S, Millard S, Soutsos M, Barnett S, Le TT. Influence of aggregate and curing regime on the mechanical properties of ultra-high performance fibre reinforced concrete (UHPCFRC). Construction and Building Materials 2009; 23(6): 2291–2298. https://doi.org/10.1016/j.conbuildmat.2008.11.012.

[116] Li B. The research on preparation of environmentally friendly ultra-high-performance concrete with low cost. PhD thesis. Hunan University; 2009.

[117] Collepardi S, Coppola L, Troli R, Collepardi M. Mechanical properties of modified reactive powder concrete. ACI Special Publication 1997; 173: 1–22. https://doi.org/10.14359/6175.

[118] Wang C, Yang C, Liu F, Wan C, Pu X. Preparation of ultra-high-performance concrete with common technology and materials. Cement and Concrete Composites 2012; 34(4): 538–544. https://doi.org/10.1016

/j.cemconcomp.2011.11.005.
[119] Sohail MG, Kahraman R, Al Nuaimi N, Gencturk B, Alnahhal W. Durability characteristics of high and ultra-high-performance concretes. Journal of Building Engineering 2021; 33: 101669. https://doi.org/10. 101 6/j.jobe.2020.101669.
[120] Wang D, Ju Y, Shen H, Xu L. Mechanical properties of high-performance concrete reinforced with basalt fiber and polypropylene fiber. Construction and Building Materials 2019; 197: 464–473. https://doi.org/10. 1016/j.conbuildmat.2018.11.181.
[121] Park SH, Kim DJ, Ryu GS, Koh KT. Tensile behavior of ultra-high performance hybrid fiber reinforced concrete. Cement and Concrete Composites 2012; 34(2): 172–184. https://doi.org/10.1016/j.cemconcomp. 2 011.09.009.
[122] Eisa AS, Elshazli MT, Nawar MT. Experimental investigation on the effect of using crumb rubber and steel fibers on the structural behavior of reinforced concrete beams. Construction and Building Materials 2020; 252: 119078. https://doi.org/10.1016/j.conbuildmat.2020.119078.
[123] Elshazli MT, Ramirez K, Ibrahim A, Badran M. Mechanical, durability and corrosion properties of basalt fiber concrete. Fibers 2022; 10(2): 10. https://doi.org/10.3390/fib10020010.
[124] Elshazli MT, Saras N, Ibrahim A. Structural response of high-strength concrete beams using fiber-reinforced polymers under reversed cyclic loading. Sustainable Structures 2022; 2: 000018. https://doi.org/10.54113/j. sust.2022.000018.
[125] Grabois TM, Cordeiro GC, Toledo Filho RD. Fresh and hardened-state properties of self-compacting lightweight concrete reinforced with steel fibers. Construction and Building Materials 2016; 104: 284–292. https://doi.org/10.1016/j.conbuildmat.2015.12.060.
[126] Yoo D-Y, Banthia N, Yoon Y-S. Effectiveness of shrinkage-reducing admixture in reducing autogenous shrinkage stress of ultra-high-performance fiber-reinforced concrete. Cement and Concrete Composites 2015; 64: 27–36. https://doi.org/10.1016/j.cemconcomp.2015.09.005.
[127] Afroughsabet V, Biolzi L, Ozbakkaloglu T. Influence of double hooked-end steel fibers and slag on mechanical and durability properties of high performance recycled aggregate concrete. Composite Structures 2017; 181: 273–284. https://doi.org/10.1016/j.compstruct.2017.08.086.
[128] Han J, Shui Z, Wang G, Sun T, Gao X. Performance evaluation of steam-cured HPC pipe piles produced with metakaolin-based mineral additives. Construction and Building Materials 2018; 189: 719–727. https://d oi.org/10.1016/j.conbuildmat.2018.09.044.
[129] Ma G, Li H, Wang J. Experimental study of the seismic behavior of an earthquake-damaged reinforced concrete frame structure retrofitted with basalt fiber-reinforced polymer. Journal of Composites for Construction 2013; 17(6): 04013002. https://doi.org/10.1061/(ASCE)CC.1943-5614.0000413.
[130] Nepomuceno MC, Pereira-de Oliveira L, Pereira SF. Mix design of structural lightweight self-compacting concrete incorporating coarse lightweight expanded clay aggregates. Construction and Building Materials 2018; 166: 373–385. https://doi.org/10.1016/j.conbuildmat.2018.01.161.
[131] He X, Pan Y-M, Caseres L, Torres R, Wise J. Assessment of aging mechanisms for concrete exposed to outdoor air and groundwater or soil in spent nuclear fuel dry storage systems. In: NACE CORROSION, NACE; 2018. https://doi.org/10.5006/c2018-11079.
[132] Mu R, Miao C, Luo X, Sun W. Interaction between loading, freeze–thaw cycles, and chloride salt attack of concrete with and without steel fiber reinforcement. Cement and Concrete Research 2002; 32(7): 1061–1066. https://doi.org/10.1016/S0008-8846(02)00746-9.
[133] Bondar D, Lynsdale C, Milestone N, Hassani N. Sulfate resistance of alkali activated pozzolans. International Journal of Concrete Structures and Materials 2015; 9: 145–158. https://doi.org/10.1007/s4006 9-014-0093-0.
[134] Peng Y, Zhang J, Liu J, Ke J, Wang F. Properties and microstructure of reactive powder concrete having a high content of phosphorous slag powder and silica fume. Construction and Building Materials 2015; 101: 482–487. https://doi.org/10.1016/j.conbuildmat.2015.10.046.
[135] Dils J, Boel V, De Schutter G. Influence of cement type and mixing pressure on air content, rheology and mechanical properties of UHPC. Construction and Building Materials 2013; 41: 455–463. https://doi.org/10 .1016/j.conbuildmat.2012.12.050.
[136] Aïtcin P-C. The durability characteristics of high-performance concrete: a review. Cement and Concrete Composites 2003; 25(4–5): 409–420. https://doi.org/10.1016/S0958-9465(02)00081-1.
[137] Colombo IG, Colombo M, di Prisco M. Tensile behavior of textile reinforced concrete subjected to freezing–thawing cycles in un-cracked andacked regimes. Cement and Concrete Research 2015; 73: 169–183. https: //doi.org/10.1016/j.cemconres.2015.03.001.
[138] Zhong R, Wille K. Material design and characterization of high-performance pervious concrete. Construction and Building Materials 2015; 98: 51–60. https://doi.org/10.1016/j.conbuildmat.2015.08. 027.
[139] Alkaysi M, El-Tawil S, Liu Z, Hansen W. Effects of silica powder and cement type on durability of ultra-high-performance concrete (UHPC). Cement and Concrete Composites 2016; 66: 47–56. https://doi.org/10.

1016/j.cemconcomp.2015.11.005.
[140] Bonneau O, Lachemi M, Dallaire E, Dugat J, Aïtcin P-C. Mechanical properties and durability of two industrial reactive powder concretes. ACI Materials Journal 1997; 94(4): 286–290. https://doi.org/10. 1435 9/310.
[141] Nawar MT, Eisa AS, Elshazli MT, Ibrahim YE, El-Zohairy A. Numerical analysis of rubberized steel fiber reinforced concrete beams subjected to static and blast loadings. Infrastructures 2024; 9(3): 52. https://doi. org/10.3390/infrastructures9030052.
[142] Liu J, Song S, Wang L. Durability and micro-structure of reactive powder concrete. Journal of Wuhan University of Technology—Materials Science Edition 2009; 24: 506–509. https://doi.org/10.1007/s11595-009-3506-1.
[143] Karakurt C, Bayazıt Y, et al. Freeze-thaw resistance of normal and high strength concretes produced with fly ash and silica fume. Advances in Materials Science and Engineering 2015; 2015: 830984. https://doi.o rg /10.1155/2015/830984.
[144] Lu Z, Feng Z-G, Yao D, Li X, Ji H. Freeze-thaw resistance of ultra-high-performance concrete: Dependence on concrete composition. Construction and Building Materials 2021; 293: 123523. https://doi.org/10.1016/j. conbuildmat.2021.123523.
[145] Sharaky I, Ahmad S, El-Azab A, Khalil H. Strength and mass loss evaluation of high-strength concrete with silica fume and nano-silica exposed to elevated temperatures. Arabian Journal for Science and Engineering 2021; 46: 1–23. https://doi.org/10.1007/s13369-021-06006-7.
[146] Islam MM, Alam MT, Islam MS. Effect of fly ash on freeze–thaw durability of concrete in marine environment. Australian Journal of Structural Engineering 2018; 19(2): 146–161. https://doi.org/10.1080/13 287982.2018.1453332.
[147] Ferraris CF. Alkali-silica reaction and high-performance concrete. NISTIR 5742. National Institute of Standards and Technology 1995. https://doi.org/10.6028/NIST.IR.5742.
[148] Thomas M. The effect of supplementary cementing materials on alkali-silica reaction: A review. Cement and Concrete Research 2011; 41(12): 1224–1231. https://doi.org/10.1016/j.cemconres.2010.11.003.
[149] Alexey B, Anna A. Efficacy of aluminum hydroxides as inhibitors of alkali-silica reactions. Materials Sciences and Applications 2013; 4: 1–6. https://doi.org/10.4236/msa.2013.412A001.
[150] Zhang M, Zhang W, Xie F. Experimental study on ASR performance of concrete with nano-particles. Journal of Asian Architecture and Building Engineering 2019; 18(1): 2–8. https://doi.org/10.1080/13467581.2019.1 582420.
[151] Wang K, Guo J, Wu H, Yang L. Influence of dry–wet ratio on properties and microstructure of concrete under sulfate attack. Construction and Building Materials 2020; 263: 120635. https://doi.org/10.1016/j. conb uildmat.2020.120635.
[152] Wen C, Zhang P, Wang J, Hu S. Influence of fibers on the mechanical properties and durability of UHPC: A review. Journal of Building Engineering 2022; 52: 104370. https://doi.org/10.1016/j.jobe.2022.104370.
[153] Mosavinejad SG, Langaroudi MAM, Barandoust J, Ghanizadeh A. Electrical and microstructural analysis of UHPC containing short PVA fibers. Construction and Building Materials 2020; 235: 117448. https://do i. org/10.1016/j.conbuildmat.2019.117448.
[154] El-Dieb AS. Mechanical, durability and microstructural characteristics of ultra-high-strength self-compacting concrete incorporating steel fibers. Materials & Design 2009; 30(10): 4286–4292. https://doi. or g/10.1016/j.matdes.2009.04.024.
[155] Chen W, Zhu H, He Z, Yang L, Zhao L, Wen C. Experimental investigation on chloride-ion penetration resistance of slag-containing fiber-reinforced concrete under drying–wetting cycles. Construction and Building Materials 2021; 274: 121829. https://doi.org/10.1016/j.conbuildmat.2020.121829.
[156] Abbas S, Soliman AM, Nehdi ML. Exploring mechanical and durability properties of UHPC incorporating various steel fiber lengths and dosages. Construction and Building Materials 2015; 75: 429–441. https://doi. org/10.1016/j.conbuildmat.2014.11.017.
[157] Khan MU, Ahmad S, Naqvi AA, Al-Gahtani HJ. Shielding performance of heavyweight UHPC against nuclear radiation. Progress in Nuclear Energy 2020; 130: 103550. https://doi.org/10.1016/j.pnucene. 2020. 103550.
[158] Zeyad AM, Hakeem IY, Amin M, Tayeh BA, Agwa IS. Effect of aggregate and fibre types on UHPC designed for radiation shielding. Journal of Building Engineering 2022; 58: 104960. https://doi.org/10.1016 /j.jobe.2022.104960.
[159] Al-Humaiqani MM, Shuraim AB, Hussain RR. Effect of compressive strength on gamma-radiation attenuation coefficients for high-performance concrete. International Journal of Engineering and Technology 2013; 5(5): 566. https://doi.org/10.7763/IJET.2013.V5.619.
[160] Gosselin C, Duballet R, Roux P, Gaudillière N, Dirrenberger J, Morel P. Large-scale 3D printing of ultra-high-performance concrete – a new processing route. Materials & Design 2016; 100: 102–109. https://doi.o rg/10.1016/j.matdes.2016.03.097.

[161] Zhang X, Li M, Lim JH, Weng Y, Tay YWD, Pham H, Pham Q-C. Large-scale 3D printing by a team of mobile robots. Automation in Construction 2018; 95: 98–106. https://doi.org/10.1016/j.autcon.2018.08.004.
[162] Liu Z, Li M, Weng Y, Wong TN, Tan MJ. Mixture design approach to optimize rheological properties for 3D cementitious material printing. Construction and Building Materials 2019; 198: 245–255. https://doi.o rg /10.1016/j.conbuildmat.2018.11.252.
[163] Tay YWD, Ting GHA, Qian Y, Panda B, He L, Tan MJ. Time gap effect on bond strength of 3D-printed concrete. Virtual and Physical Prototyping 2019; 14(1): 104–113. https://doi.org/10.1080/17452759.2018.15 00420.
[164] Kazemian A, Yuan X, Cochran E, Khoshnevis B. Cementitious materials for construction-scale 3D printing: Laboratory testing of fresh printing mixture. Construction and Building Materials 2017; 145: 639–647. https ://doi.org/10.1016/j.conbuildmat.2017.04.015.
[165] Mantawy IM, Thonstad T, Sanders DH, Stanton JF, Eberhard MO. Seismic performance of precast, pretensioned, and cast-in-place bridges: Shake-table test comparison. Journal of Bridge Engineering 2016; 21(10): 04016071. https://doi.org/10.1061/(ASCE)BE.1943-5592.0000934.
[166] Azizinamini A, Rehmat S, Sadeghnejad A. Enhancing resiliency and delivery of bridge elements using UHPC as formwork. Transportation Research Record 2019; 2673(5): 443–453. https://doi.org/10.1177/0361 198119834907.
[167] Berry M, Snidarich R, Wood C, et al. Development of non-proprietary ultra-high-performance concrete: Project summary report. Montana Department of Transportation 2017. https://doi.org/10.21949/1518196.
[168] El-Tawil S, Tai Y-S, Meng B, Hansen W, Liu Z, et al. Commercial production of non-proprietary ultra-high-performance concrete. Michigan Department of Transportation 2018. RC-1670. Source: https://www.michi gan.gov/mdot/media/Project/Websites/MDOT/Business/Research/RC1670.pdf
[169] Shokrgozar A. Bond strength behavior between non-proprietary UHPC and high-strength precast concrete bridge components. PhD Thesis. Idaho State University 2023.